applied sciences

MDPI

Article

A Robust Generator–Harvester for Independent Sensor Systems †

Jiří Zukal, Zoltán Szabó, Tomáš Kříž, Radim Kadlec, Jamila Dědková and Pavel Fiala *

Department of Theoretical and Experimental Electrical Engineering, Brno University of Technology, Technická 12, 616 00 Brno, Czech Republic; 223365@vut.cz (J.Z.); szaboz@vut.cz (Z.S.); krizt@vut.cz (T.K.)

* Correspondence: fialap@vut.cz; Tel.: +420-604-076-280

† This paper is an extended version of our paper published in PIERS 2023 conference, Zukal, J.; Szabo, Z.; Pernica, R.; Kadlec, R.; Dedkova, J.; Klima, M.; Fiala, P. Designing a Robust Model of a Linear Motion-driven Harvester. In Proceedings of the 2023 Photonics & Electromagnetics Research Symposium (PIERS), Prague, Czech Republic, 3–6 July 2023, pp. 732–738, https://doi.org/10.1109/PIERS59004.2023.10221336.

Abstract: The research is centered on energy production and harvesting to facilitate the transformation of electrical energy with energy-independent sensor systems, using powering devices in the expected power range of P = 10–10,000 W. A model application case for a harvester is the conversion of energy stored in the compressed gas during expansion; such gas embodies the energy stored in scenarios such as braking a car using an auxiliary pump. Similar systems find use in sensing various quantities in the transport sector (bridge structures, infrastructural components, cars, and other objects). The proposed theoretical harvester models describing the transformation of linear motion energy into electricity provide relevant support for the experiments. In the given context, the results obtained in the designing and construction of a robust motion generator with a primarily linear geometry-based system technology are presented, too. The expected output of electrical power of an N-segment harvester within the tested type is variable, and the design exploits the rectilinear motion generated by an engine using compressed air, a small fuel system, and similar options to obtain an expected/adjustable N-segment power in the range of P_{sm} = 10–500 W. The fundamental structure of the generator core has been continuously numerically modeled, and an experimental setup has been developed to analyze the specific parts and variations in order to validate the concept and to achieve the most suitable parameters with the selected construction materials (a power yield increase of up to 2000 times). A scaled-down version of the model principle was tested in the experiments, and the parameters and results were compared with the predicted theoretical analyses. Generally, the conceptual layout of an enhanced magnetic circuit layout transforming motion energy into electricity was presented and verified.

Keywords: harvesting; electromagnetic field; numerical model; renewable energy; linear motion; sensor systems

Citation: Zukal, J.; Szabó, Z.; Kříž, T.; Kadlec, R.; Dědková, J.; Fiala, P. A Robust Generator–Harvester for Independent Sensor Systems. *Appl. Sci.* **2024**, *14*, 1246. https://doi.org/10.3390/app14031246

Academic Editor: Alessandro Lo Schiavo

Received: 13 November 2023
Revised: 8 January 2024
Accepted: 15 January 2024
Published: 2 February 2024

1. Introduction

Between the years 2000 and 2020, the trends of energy saving, energy system independence, energy processing efficiency, and energy harvesting based on electromagnetic field principles [1] reached almost all industries. The field of energy harvesting, or the concept of energy transduction [2–4], does not cover the entire area of energy production and processing to convert diverse forms of energy into electricity; this domain includes only a limited part of the principles [5–8] and corresponding device designs [9–12] that allow exploiting unused types of energy for a given purpose [13,14]. In power generation, specific energy conversion principles still remain to be included, such as the conversion of energy from flowing media (water, air) and the conversion of incident RF electromagnetic waves, namely, photovoltaic systems, into electricity [15–17].

Considering the scarcity of alternative energy sources, these may find application mainly in mobile or wireless devices [18–20], sensor-independent systems [3,4], autonomous

sensor instruments, and systems where a stable power supply is disadvantageous or impossible to secure [3,4]. The requirement for the development and use of alternative energy source principles involves, among other factors, estimating the minimum operating time without a stable/permanent (non-mobile) distribution system.

A narrower, more tightly defined segment of power harvesting and generation utilizes Faraday's law of induction [1] in devices that employ vibration [3], rotational motion, and/or linear motion [2,4–6]. These principles are further modified through various concepts of micro-, mini- [3], and large-sized generators [2]. In the last-named option, the power delivered is expected to be in the order of tens to thousands of watts, either discontinuously or in a continuous time. Such generators and design approaches must meet the desired lifetime requirements, and if they satisfy this prerequisite, they are referred to as robust.

Designing conceptual solutions to enable a highly efficient conversion of motion into electrical energy is an interesting—and already partially solved—problem. The principle of converting motion energy into electricity is based on the understanding and consistent use of the possibilities of Faraday's induction law [1], as presented in sources [3,4] and [18–20] and as outlined hereabove.

Researching and exploring suitable harvester concepts are steps that generally allow us to identify a highly efficient device to transform kinetic energy, potentially enabling the operator to power components such as sensors with permanently supplied electrical energy that may be of rare origin. In sensors and measuring systems, special transportation equipment, and cars, meaning items that feature a higher power consumption (P = 10–1000 W), the power supply of electricity from conventional sources such as batteries, internal combustion engines, and related sources is either disadvantageous in terms of the solution and cost or difficult to implement. For this reason, residual or alternative forms of energy are then widely sought for, including, but not limited to, the expansion of compressed air and various types of linear movement. The options of converting kinetic energy into electricity comprise, for example, the electromagnetic principle based on the full Faraday effect, the result being high conversion efficiency [1,18–20].

The project presented herein expands on the concepts in paper [21], namely, efficient methods for generating and exploiting linear motion. In this article, however, the parameters of selected vibration harvesters are discussed and compared in greater detail, and, importantly, an estimation the expected characteristics inherent with the proposed implementation is outlined. Further, the relevant numerical model based on Maxwell's equations is rendered more extensively, both in the derivation and the results, and can be applied using powerful numerical modeling tools in the Finite element system The novel, expanded diagrams that display three experimentally tested concepts of one cell of the periodic arrangement of the harvester, then allow us to represent the symbolic connection of the magnetic circuit in one element of the harvester and express the periodic structure of the experimental generator. The practical measurements centered on three novel configurations of the magnetic circuit then show that a suitably arranged harvester cell circuit facilitates in achieving a major increase in the movement energy extraction (up to 2000 times the power obtained under comparable electrical load setting conditions). These experiments and evaluation tasks have been performed to refine and verify the previous outcomes. Regarding the conference paper "Designing a Robust Model of a Linear Motion-driven Harvester", the authors showed how changing the arrangement of the magnetic circuit can fundamentally affect the output parameters, namely, the produced electricity yield; this step was carried out by measuring along the outlines of the documented experiment.

To the best of our knowledge, no extensive research on designing the magnetic circuit in linear generators to achieve the maximum possible rate in converting motion energy into electricity has been conducted to date. To facilitate such work, it is necessary to know the principle and mathematical model that lead to formulating the coupling and energy conversion as well as the technological feasibility of the design (detail of the magnetic flux

changes). A large portion of the tasks is nevertheless proposed in this article, which thus may support further development in the field.

2. State of the Research Field and Topics Analyzed

We discuss the designing and selection of a concept to convert various forms of energy into electromagnetic energy, the central aim being to transform mechanical linear motion into electricity. In this context, a broad range of approaches are examined to yield instantaneously delivered/transmitted electrical power in the range of P = 10–10,000 W. The published articles and papers can be classified into several groups. The first one embraces the area of designing and solving the electrical, electronic, and electromagnetic parts of the projected devices; prominent sources include, above all, [5–8]. Another group addresses the harvester/generator drive issues, often in relation to combustion engine functions and parts [9–12]. Yet, another set comprises articles on motion generation, the drifting of the electromagnetic part of the generator [13,14], models [18–20], motion principles, and appropriate experiments [22–37]. Further categories cover the following methods and processes, respectively: the linear motion of the power unit based on the hydraulic transfer of dynamic energy to the motion element within the linear generator configuration, the generator system (kinetic-to-electrical energy conversion) and the control, modeling, simulation, measurement, and evaluation of relevant model parameters.

Detailed insights into the analysis and solution of the generator concept and more serious attempts to create a mathematical model and simulation of the hybrid motor are provided in, for example, articles [38,39], which focus on designing the purely electromagnetic part, i.e., on electromagnetic conversion using a generator. Another research direction leads to the designing and solution of the combustion power unit in linear engines, namely, an engine with free pistons. This mechanism, relative to a rotary engine with a crank mechanism, has only one or two pistons connected on a common shaft [26] and features precisely the controlled detonation and dynamics of the moving mass. A linear motor with free pistons uses the motion of a common shaft, on which a linear electric generator is mounted [40], or, alternatively, a hydraulic piston mounted on a common shaft is employed to generate hydraulic pressure by moving the piston. Only a limited number of authors [41] have hitherto simulated a setup to control a motor with a hydraulic pump.

The publications, to date, on the construction and testing of a linear combustion engine in connection with a generator include articles and theses from West Virginia University (the USA) [2,4], in which using the engine is also considered for an electric power generator applicable in relatively remote locations, thanks to fewer moving parts and greater reliability, efficiency, and compactness [5] compared to the rotary engine concept. Similarly, the authors of [6,42] propose employing a linear combustion engine as an electric power generator to replace the current gasoline or diesel generators. By extension, the basic areas that host linear generators in conjunction with a free-piston internal combustion engine subsume automotive technologies and independent power systems. The basic elements of a linear generator are a linear internal combustion or a free-piston engine and a linear electric motor generating electrical energy (linear generator).

The requirements of a linear electric generator resulting from a basic analysis of a linearly arranged internal combustion engine with a generator, all in terms of the output power achieved for charging the traction battery Q = 21 kWh and the electric drive P = 80 kW, are published in [43]. Other published articles or papers discuss, for instance, an approach that relies on deploying a linear generator to convert the mechanical vibrations of a car into electrical energy [44]. Some of the researchers also analyze the performance and quality of a linear microgenerator, including testing to exploit the energy from the mechanical propagation of waves with free pistons [7].

2.1. Problems Relating to the Electromagnetic Component of the Designed Harvester

A specific area of research within the above power generation procedures encompasses the designing of the electromagnetic part of the device or apparatus, completed with

associated steps and stages such as coupling to a motion source and interaction with the system that is being powered, namely, a sensor or a sensor system. A detailed discussion of linear machine concepts suitable for use in linear motor/generator configurations, including an interpretation in terms of the geometry (planar or tubular), is available in [22]. A comparison involving linear generators is detailed in [23].

Furthermore, an interesting area lies in modeling specifically designed devices, as is presented in articles [24,25].

The decisive parameter for comparing the efficiency of the design and implementation of generators and their transformation characteristics, the parameters for the choice of the downstream concept, is the quantity effective volumetric power density p_{efd} [W/m^3], shown in Table 1 [20]. Using this parameter, the efficiency rates of an energy source with respect to its volume are easily comparable, and such a procedure thus facilitates the comparison between selected concepts and designs, which may be dimensionally different and difficult to measure.

Table 1. The parameters of selected mini-generators Reprinted/adapted with permission from Ref. [20]. Copyright 2024, copyright Pavel Fiala [20].

Reference	Permanent Magnet Type	Generator Body Size x,y,z [m]	Output Power P_{out} [W]	Output Voltage U_{out} [V]	Effective Power Density p_{efd} [W/m^3]
Beeby et al. [28], 2007	–	375 mm^3	2×10^{-6}	0.428 RMS	≈6
Zhu et al. [29], 2010	FeNdB	2000 mm^3	$61.6–156.6 \times 10^{-6}$	–	≈30−80
Kulkarni et al. [27], 2008	FeNdB	3375 mm^3	0.6×10^{-6}	0.025	≈0.2
Wang et al. [31], 2007	FeNdB	256 mm^3	-	0.06	-
Lee et al. [33], 2012	FeNdB	1.4×10^{-4} m^3	1.52×10^{-3}	4.8	≈10
Yang et al. [32], 2014.	–	50,000 mm^3	13.4×10^{-3}	0.7−2.0	≈270
Elvin et al. [30], 2011	–	15,000 mm^3	4×10^{-6}	0.007	≈0.26
MG I [18], 2006	FeNdB	90, 40, 30 mm	70×10^{-3}	4−60 (300) p-p	≈650
MG II [18], 2006	FeNdB	50, 27, 25 mm	19.5×10^{-3}	6−15	≈60
MG III	FeNdB	50, 25, 25 mm	5.0×10^{-3}	1.0−2.5	≈15
MG IV	FeNdB	50, 35, 25 mm	8.0×10^{-3}	1.0−2.5	≈18
* Lith. battery [34], 2018	* Lith. battery				≈40×10^6
* Supercap [35], 2010	* Supercap				≈3−5
* Fuel	* Fuel				≈4×10^9
* U_{235}	* U_{235}				≈9×10^{16}

The asterisk indicates a note for conventional energy sources (batteries, fuel, nuclear reaction) for comparison with harvesters.

2.2. Designing an Electromagnetic Transformation Method: Renewable Energy

The first article written by prominent researchers in linear motion generation was published at West Virginia University [4], focusing on the engine and alternator sections.

The direct design of a linear synchronous generator and the magnetic flux density distribution via a finite element analysis are outlined in [36]. The generator consists of a stator that comprises coils and a rotor made of permanent magnets.

3. Mathematical–Physical Model

The basic formulation for deriving the mathematical expression to characterize the electromagnetic part of the model is based on Faraday's induction law (1); see, for example, the interpretation by J.A. Stratton [1]. The use of 3D modeling and simulation, analysis, and comparisons with experimental models of a linear generator is discussed in multiple sources, including [8,18–20]. The simulation and experimental verification of the parameters of the equivalent circuits and the rotor/stator core losses via the FEM are addressed in article [37]. An evaluation of the related impact of the electrical parameters, load, and drive dynamics is proposed in [7,8].

According to [8,20], the change in the magnetic flux Φ according to Faraday's induction law is

$$\underbrace{\oint_{\ell} \boldsymbol{E}(t) \cdot d\ell}_{\Phi} = -\int_{S} \frac{\partial \boldsymbol{B}(t)}{\partial t}\, dS + \oint_{\ell} (\boldsymbol{v}(t) \times \boldsymbol{B}(x,y,z,t)) \cdot d\ell, \quad (1)$$

where $\boldsymbol{E}$(t) is the electric field intensity vector, $\boldsymbol{B}$(t) denotes the magnetic flux density vector (induction), $\boldsymbol{v}$(t) indicates the speed of the shift of the generator core position in time (instantaneous speed), S denotes the cross-section of the magnetic flux regions, and λ denotes the curve along the boundary of area S.

The simple concept, which was experimented with previously [2–4,8,20], can be applied to the electromagnetic part of the harvester. The equation of the motion relating to the arrangement of the electromagnetic part of the generator/harvester, the force field couplings, and the linear motion of the moving part are expressible as

$$m\ \ddot{x} + l_c\ \dot{x}\ + k\ x = f_{mag}(B, \dot{x}, t) + f_{mech}(t), \quad (2)$$

where m is the mass, m_m denotes the mass of the moving part of the generator system, l_c is the damping coefficient, k represents the stiffness coefficient, x stands for the position of the body, $\dot{x}$ expresses the velocity of the moving part (dx/dt), $\ddot{x}$ is the acceleration of the moving part (d^2x/dt^2), f_{mag} stands for the force acting on the moving part via interaction with the magnetic field, and f_{mech} denotes the force of the mechanical motion of the moving part of the linear actuator.

In order to obtain a concept to deliver an efficient harvester yield with linear motion, we have to accept the dynamic parameters of the system to prevent the the conceptual design from markedly reducing the energy conversion efficiency of the generator system already at the beginning of the actual designing task. As already determined via a comparison with other motion/vibration harvester designs [20], the moving segment of the electromagnetic part of the generator for the zenith linear actuator concept must, in the moving part, exhibit a mass parameter m_m close to the minimum value (solution of Equation (2), Figure 1a). In the case of the moving part of the generator model, the mass must be close to the minimum. The instantaneous value of the electric current through the winding i(t) at an electric load on the terminals of the winding R_z can be derived and formulated according to the procedure in [2].

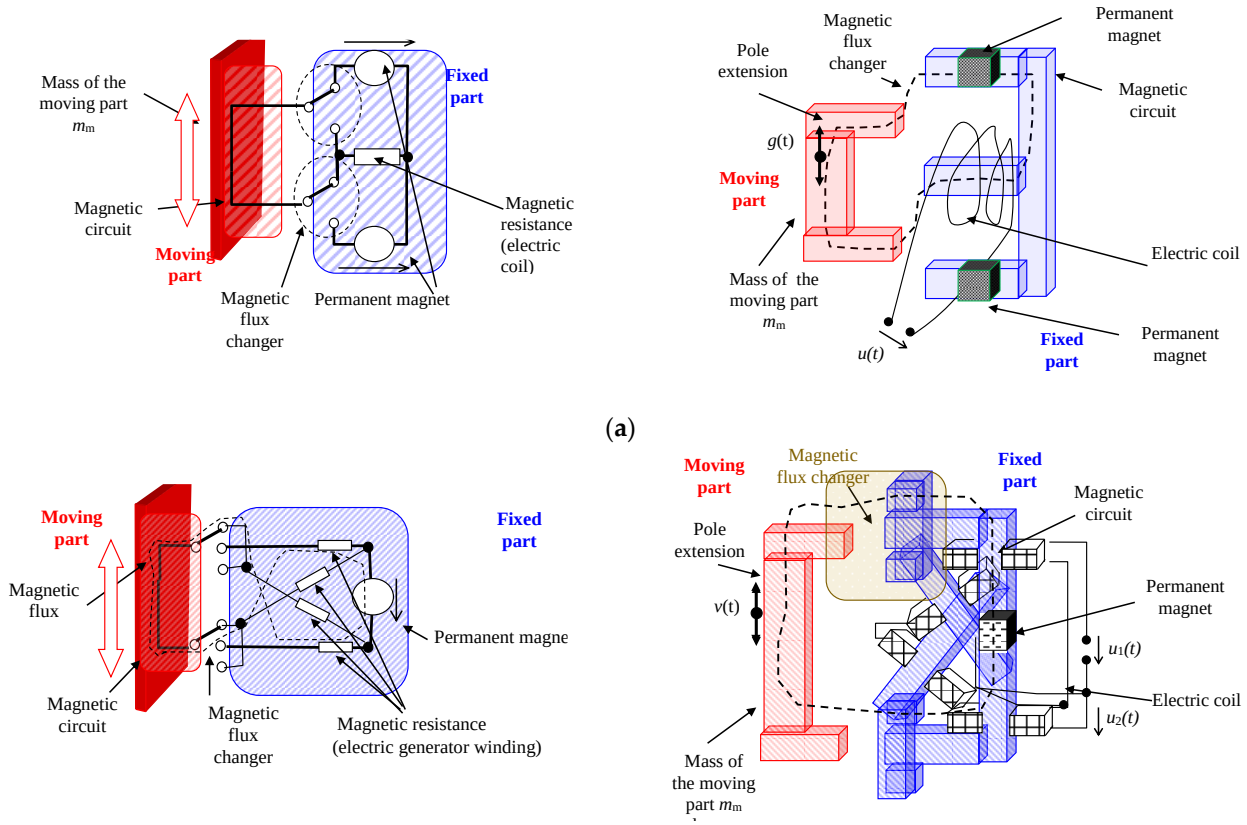

Figure 1. (**a**) A modified magnetic circuit: a model with concentrated parameters (left) and its design scheme (right) in a linear motion system with minimized dynamic losses (double-acting arrangement). (**b**) A modified magnetic circuit: a model with concentrated parameters (left) and its design scheme (right), representing an arrangement for the maximum yield efficiency of the linear motion system with minimized dynamic losses (a double-acting arrangement).

If the electromagnetic arrangement of a linear generator is considered, as shown in, for example in [36], it will be driven by the corresponding unit (an internal combustion engine) in the dynamic non-volatile state (2); to characterize such an application, we employ a general mathematical model.

Faraday's law of induction (1) is employed to formulate the principle and the design of the active part of the generator, also enabling the motion energy of the system to transform into electrical energy, through induction, to the electrical voltage in the inserted conductor of the electric winding; the relevant part is described as

$$\oint_{\ell} E(t) \cdot dl = -\frac{d\Phi(t)}{dt} \tag{3}$$

If a thin conductor in the form of a closed loop is inserted into such a variable electric field, an electric current i(t) starts to flow therein. Now, let us denote the current that flows through the closed loop without the presence of an external source of electric voltage as the induced current. The magnetic flux Φ is generated by an external magnetic field. We then have

$$u(t) = -\frac{d\Phi(t)}{dt} \tag{4}$$

$$u(t) = u_1(t) + u_2(t) \tag{5}$$

$$u(t) = U_{mag}|g(t)| \tag{6}$$

where U_{mag} is the maximum value of the induced coil winding voltage for a single-line arrangement (Figure 1a) under the given conditions, and g(t) denotes a function of the time dependence of the magnetic field corresponding to the system parameters and the dynamics of the moving part of the generator. The resulting induced voltage for the double-acting arrangement (Figure 1b) changes with respect to the single magnetic circuit arrangement into the form (6).

The energy stored in the magnetic field source (a permanent magnet) is written as

$$W_m = \int\limits_{V_m} \frac{1}{2} B_M H_M \, dV, \tag{7}$$

where B_{M}, H_{M} are the magnetic flux density and magnetic intensity at the working point of the permanent magnet, and V_{m} denotes the volume of the magnet. The energy, converted into heat (Joule heat), in the winding of the loaded coil (for our problem, an irreversible form of energy) reads

$$W_J = \int\limits_{V_{Jc}} \frac{1}{2} \frac{J^2}{\gamma} \, dV, \tag{8}$$

where γ is the specific conductance of the coil conductor, $\boldsymbol{J}$ represents the current density vector, and V_{Jc} represents the volume of the coil conductors. The energy that dampens the moving oscillatory motion of the generator core due to the electrical load on the coil terminals is written as

$$W_V = \int\limits_{\ell} \int\limits_{V_J} f_m \, dV \cdot \boldsymbol{n} d\ell = \int\limits_{\ell} \int\limits_{V_J} (\boldsymbol{J} \times \boldsymbol{B}) \, dV \cdot \boldsymbol{n} d\ell \tag{9}$$

where f_{m} is the specific force acting on the motion part of the generator, $\boldsymbol{n}$ stands for the normal vector in the direction of the electric current flow i(t), dλ denotes the displacement length due to the specific force, $\boldsymbol{B}$ is the magnetic flux density vector, and V_{J} expresses the volume of the electrically conductive components. From Equations (7)–(9), the equation of state is obtained as follows:

$$m_m \, a \, dx - \int\limits_{\ell} \int\limits_{V_J} (\boldsymbol{J} \times \boldsymbol{B}) dV \cdot \boldsymbol{n} d\ell - \int\limits_{V_{Jc}} \frac{1}{2} \frac{J^2}{\gamma} \, dV = \frac{1}{2} m \left(\frac{d \, x}{dt} \right)^2, \tag{10}$$

$$\eta \int\limits_{V_m} \frac{1}{2} B_M H_M dV = \frac{1}{2} m_m \left(\frac{d \, x}{dt} \right)^2, \tag{11}$$

where dx is the deflection of the generator core, η represents the energy utilization efficiency of the permanent magnet module, and a denotes the acceleration ($\mathrm{d}^2x/\mathrm{d}t^2$). After being modified, and when the expressions for voltage and current have been inserted, Equation (11) reads

$$m_m \, a \, dx - \int\limits_{\ell} \int\limits_{V_J} \left(\frac{I}{S_v} \boldsymbol{n} \times \boldsymbol{B} \right) dV \cdot \boldsymbol{n} d\ell - \int\limits_{V_{Jc}} \frac{1}{2} \frac{\left(\frac{I}{S_v} \right)^2}{\gamma} \, dV = \frac{1}{2} m_m \left(\frac{d \, x}{dt} \right)^2, \tag{12}$$

$$\eta \int\limits_{V_m} \frac{1}{2} B_M H_M dV = \frac{1}{2} m_m \left(\frac{d \, x}{dt} \right)^2, \tag{13}$$

where I is the maximum value of the amplitude of the electric current flowing through the coil conductor, S_v is the cross-section of the winding conductor, and dt is the time change. Then, we have

$$m_m\, a\, dx - \int_{\ell}\int_{V_J}\left(\frac{P}{U\, S_v}\boldsymbol{n}\times\boldsymbol{B}\right)dV\cdot\boldsymbol{n}d\ell - \int_{V_{Jc}}\frac{1}{2}\frac{\left(\frac{P}{U\, S_v}\right)^2}{\gamma}\, dV = \frac{1}{2}m_m\left(\frac{d\, x}{dt}\right)^2 \tag{14}$$

By comparing Equations (12)–(14), an expression is obtained from which the order of magnitude of the moving part (core) of the generator can be determined depending on the pre-specified parameters.

$$m_m\, a\, dx - \int_{\ell}\int_{V_J}\left(\frac{P}{U\, S_v}\boldsymbol{n}\times\boldsymbol{B}\right)dV\cdot\boldsymbol{n}d\ell - \int_{V_{Jc}}\frac{1}{2}\frac{\left(\frac{P}{U\, S_v}\right)^2}{\gamma}\, dV = \eta\int_{V_M}\frac{1}{2}B_M H_M\, dV \tag{15}$$

According to Equations (2)–(14), the addition of the braking forces F_{br} gives the basic formula that characterizes the generator system. We have

$$\begin{aligned}
m\frac{d^2x}{dt^2} + l_c\frac{dx}{dt} + k\,x &= m_m\frac{d^2x}{dt^2} - \underbrace{\int_{V_J}(\boldsymbol{J}_v\times\boldsymbol{B})\cdot\boldsymbol{n}\, dV}_{F_{br}} - \int_{V_{Jc}}(\boldsymbol{J}_{circ}\times\boldsymbol{B})\cdot\boldsymbol{n}\, dV,\\
m\frac{d^2x}{dt^2} + l_c\frac{dx}{dt} + k\,x &= m_m\frac{d^2x}{dt^2} - \int_{V_J}\left(\left(\frac{dx}{dt}\boldsymbol{u}_x\times\boldsymbol{B}_{br}(t)\right)\times\boldsymbol{B}\right)\cdot\boldsymbol{n}\, dV - \int_{V_{Jc}}\left(\frac{i(t)}{S_v}\boldsymbol{n}\times\boldsymbol{B}\right)\cdot\boldsymbol{n}\, dV,\\
m\frac{d^2x}{dt^2} + l_c\frac{dx}{dt} + k\,x &= m_m\frac{d^2x}{dt^2} - \int_{V_J}\left(\left(\frac{dx}{dt}\boldsymbol{u}_x\times\boldsymbol{B}_{br}(t)\right)\times\boldsymbol{B}\right)\cdot\boldsymbol{n}\, dV - \int_{\ell_{Jc}}(i(t)\boldsymbol{n}\times\boldsymbol{B})\cdot\boldsymbol{n}\, d\ell,
\end{aligned} \tag{16}$$

where $\boldsymbol{B}_{\mathrm{br}}$ is the braking component of the magnetic induction vector, $\boldsymbol{J}_{\mathrm{v}}$ denotes the current density vector of the electrically conductive components due to eddy currents, $\boldsymbol{J}_{\mathrm{circ}}$ represents the current density vector in the coil winding, i(t) stands for the instantaneous value of the coil electric current, and $\boldsymbol{u}_{\mathrm{x}}$ is the unit vector of the coordinate system. Interestingly, in this context, the approaches described in research articles [45,46] can be considered inspiring for further characterization of the modeling procedure.

The model described above was compiled using the finite element method (FEM) in ANSYS [47]. Both the dynamics of the model in the Ansys Multiphysics module [47] and the magnetic field distribution subproblems for the static and the quasi-stationary arrangements were analyzed, as shown below

To increase the yield (efficiency) of the dynamic energy transformation (Figure 1a) generated by the motion, the magnetic circuit layout, according to Figure 1b, is applicable.

In order to achieve a high efficiency in the Faraday induction law-based conversion (1) of the kinetic energy of the generator into electricity, the arrangement of the magnetic circuit, shown schematically in Figure 1a, is utilized. Due to the arrangement of the magnetic circuit in Figure 1b, the change in the flux dΦ/dx or dΦ/dt in Figure 1b is multiplied. A significant increase in the magnitude of the induced electric voltage u(t) can therefore be expected in a comparable winding of the electric generator. This corresponds to a change in the proposed arrangement (Figures 2 and 3) for the resulting electric voltage u(t). The segment of the magnetic arrangement of the linear generator will be periodically repeated during the designing part, and therefore the sections and subchapters below will deal with the fundamental parts of the periodic arrangement of the generator elements.

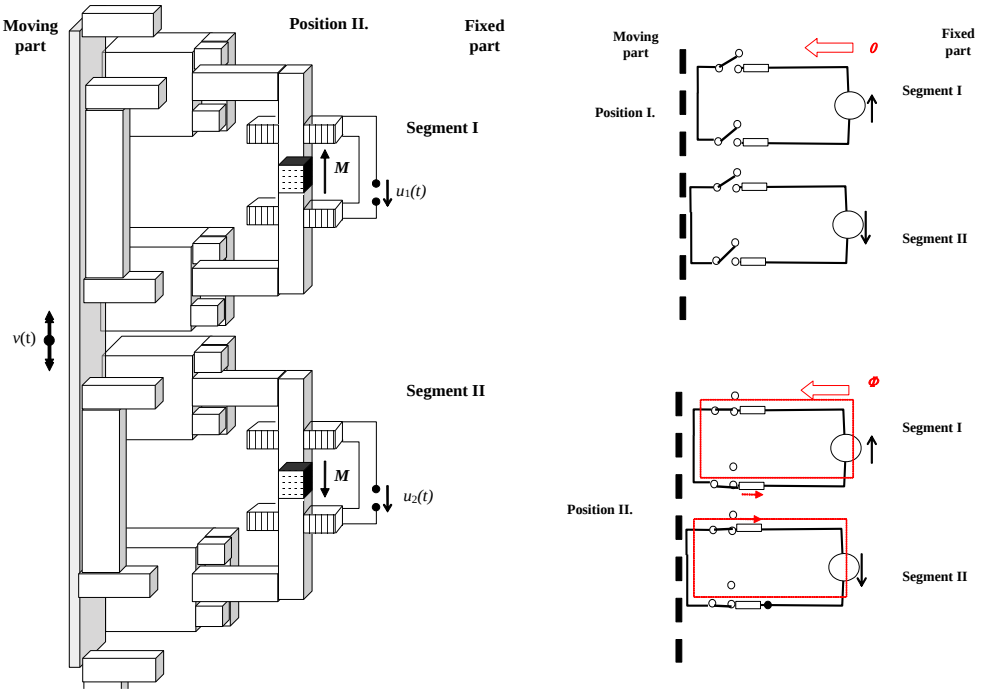

Figure 2. The segments I and II of a single-acting magnetic circuit arrangement of the periodic structure of the linear motion shown below. Such configurations allow us to achieve the maximum change in the magnetic flux of the moving and fixed parts: (**a**) a principal geometrical arrangement, and (**b**) a symbolic representation of the magnetic circuit (a model with concentrated parameters).

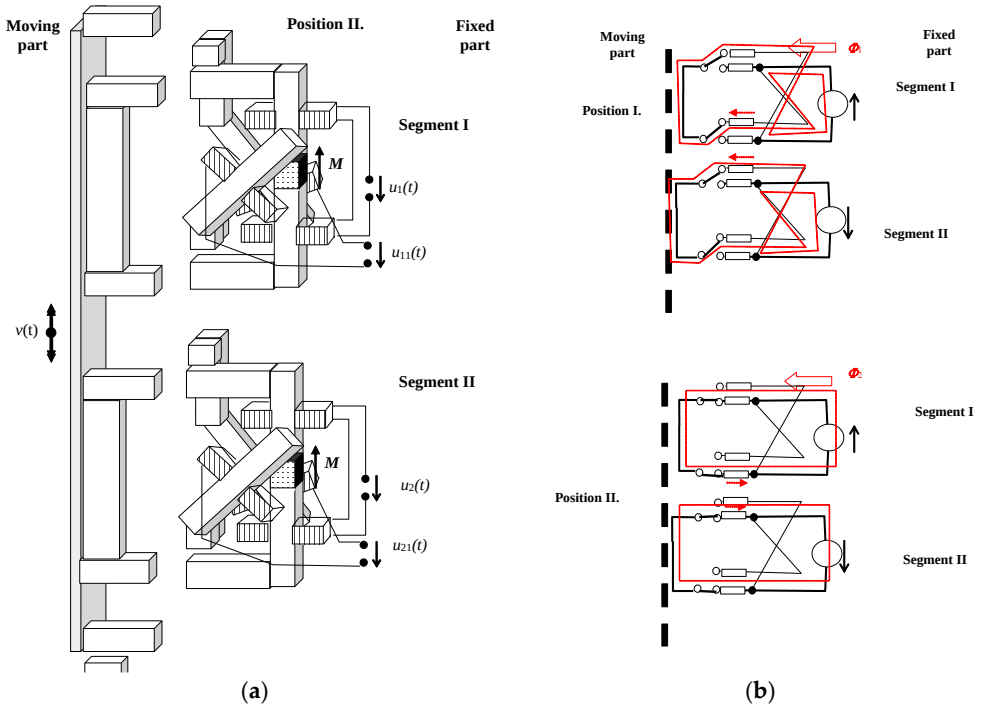

Figure 3. The segments I and II of the double-acting magnetic circuit of the periodic structure of the linear motion to achieve the maximum change in the magnetic flux of the moving and fixed parts: (**a**) principal geometrical arrangement, and (**b**) a symbolic representation of the magnetic circuit (a model with concentrated parameters).

The magnetic circuit arrangement and efficiency are related to the arrangement of the transition of the moving part of the magnetic circuit to the circuit of the fixed part of the generator. The detail is provided in Figure 1b—magnetic flux converter. Several pole mounting configurations for transmitting the magnetic flux through the air gap of the moving and the static parts of the generator are illustrated in Figure 4.

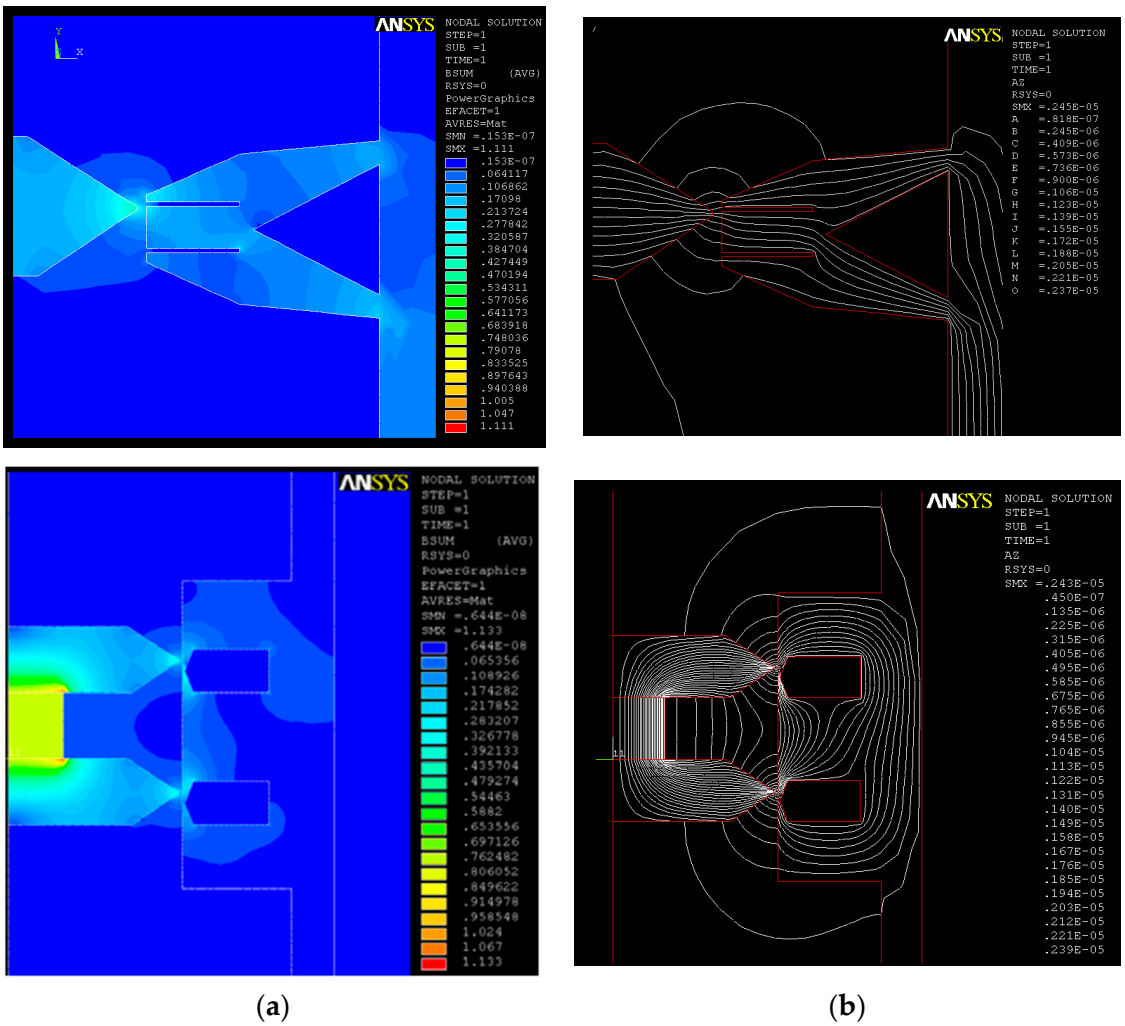

(**a**) (**b**)

Figure 4. Examples of pole attachment geometry FEM solutions, single- or double-acting models: (**a**) the magnetic flux modulus *B*, and (**b**) the fluxlines l in the detailed design of a magnetic flux converter.

4. Experiments

Considering the previously published approaches referred to above, especially in the introduction, an experimental concept of a generator with a renewable form of energy and a linear displacement-driven generator (compressed gas [38]), we proposed the specific arrangement shown in Figure 2. The renewable form of energy in compressed gas is considered in car-based transportation systems that perform braking via compressing air into a container, the air being subsequently used as "renewable energy", or, by a more exact definition, extracted from the energy during braking, engine starting, and other relevant action. The concept employs two piston units (Figure 5b,c) driven by CO_2 or N_2, which are adapted from a CO_2 engine (Figure 5a). The power unit and the link to the electromagnetic generator are schematically represented in Figure 5b. The theoretical properties of the magnetic flux transition from the moving to the fixed part of the magnetic circuit through air (Figure 4) were utilized in the design of the experimental embodiment (Figure 5d) of the

generator concept, comprising both the single-acting and the double-acting embodiments (Figures 3 and 4, respectively). Figure 6 shows the single-segment setup for the experimental verification concept of the single-acting generator design (Figure 2). Figure 5c then details the full setup of the experimental fixture with four segments, in the single-acting design (Figure 2), and the setup for the load mode test $Z_{1,Re}$ = 150 Ω, $Z_{2,Re}$= 1000 Ω, and $Z_3 = \propto \Omega$.

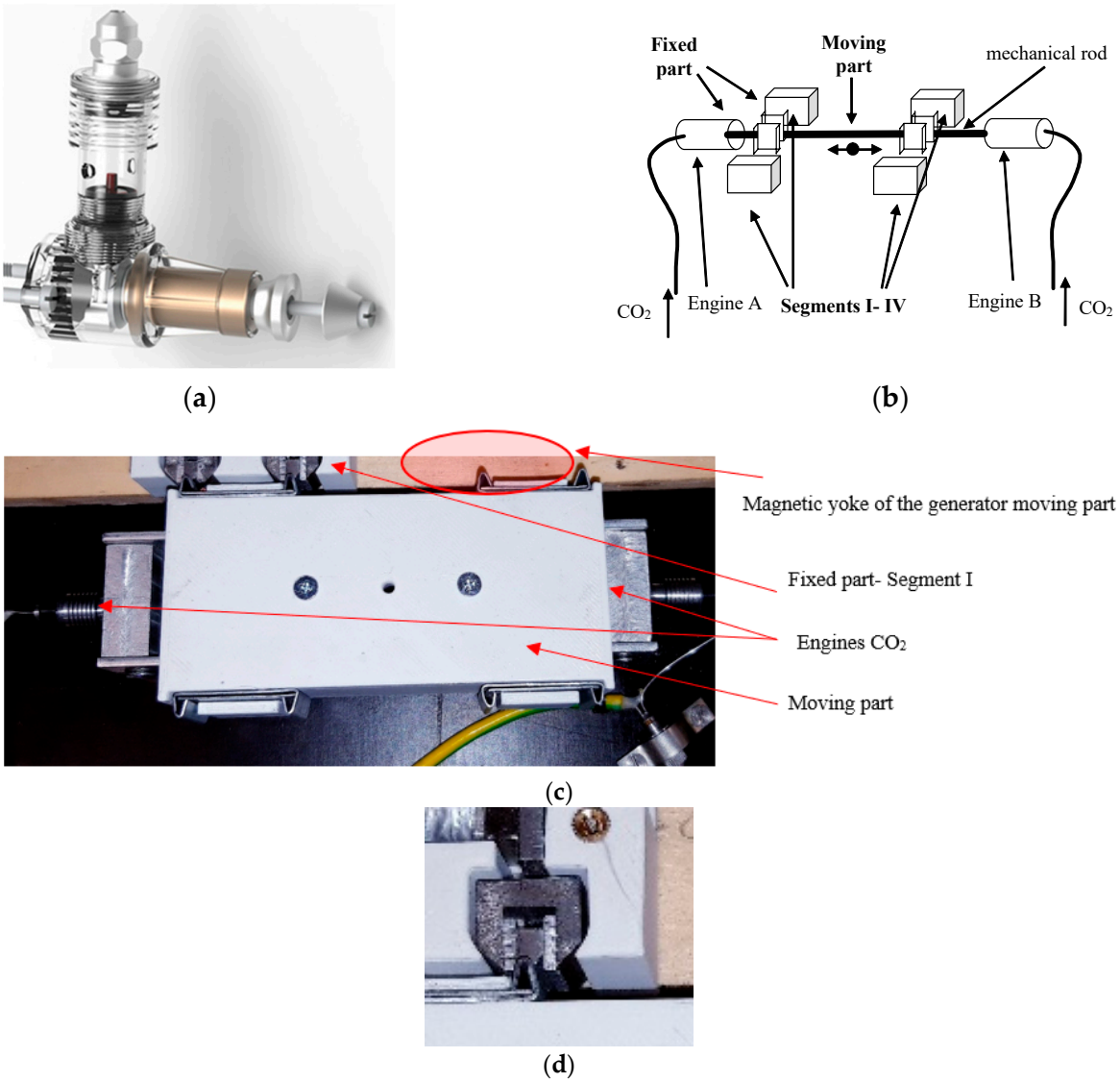

Figure 5. The linear generator drive unit: (**a**) CO_2 engine, (**b**) unit arrangement, (**c**) experimental arrangement, (**d**) detail of the pole adapter—flux converter of segment I (the concept from Figure 2).

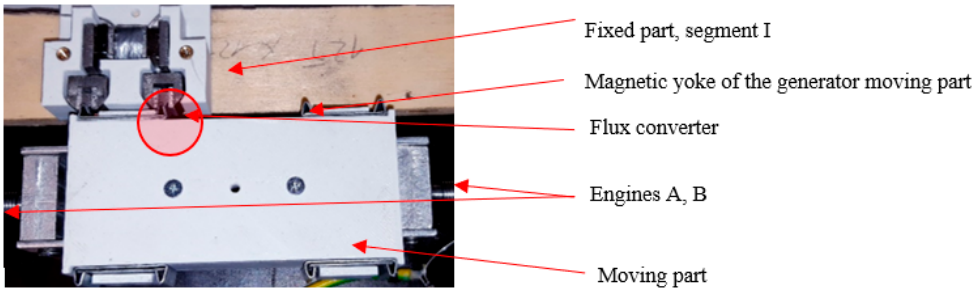

Figure 6. The experimental part (one segment) of the verification of the single-acting variant of the harvester, type I, type II.

The windings of the coils with turn N_1, N_2, …, N_4 of the experimental generator are connected in series with, in one sense, polarity of the output voltage on the coil. In segment I, the number of the coil turns was N_1 = 1000, and the linear motion speed equaled v = 4 m/s. The unit was driven by compressed gas N_2 at a pressure of p = 10 bar (Figure 7), and m_m = 150 g according to Equations (14)–(16). A comparison of the measurements for one module of concepts I to III (Figures 1–3) is shown in Table 2. The measuring tasks in Table 2 were performed with an oscilloscope in real time, and the mean value of the quantity was subtracted from the preset steady values. The amount of the measurements was greater than n = 30. The type A uncertainty is attached. Below (Figure 8), we show the concept of a periodic arrangement of the harvester from segments with expected parameters that meet the desired power (in the band P = 10–10,000 W) while maintaining the resistance and lifetime prerequisites, meaning a robust approach and device.

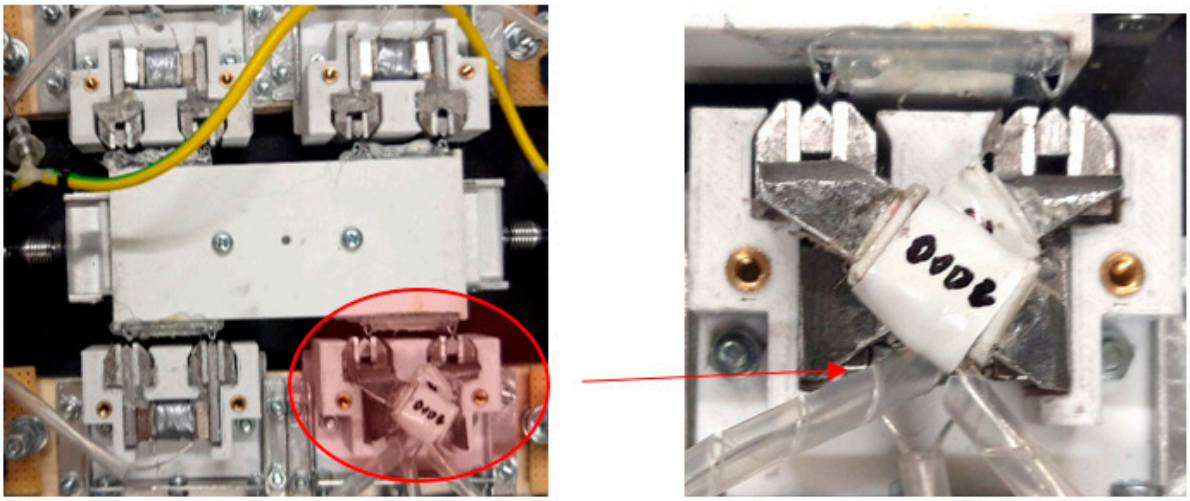

Figure 7. The experimental part of verifying (**a**) of the double-acting principle arrangement (**b**) of one segment of the harvester, Figure 2, type III.

Table 2. Comparing the basic measurements of the conceptual layout I-III with the type A uncertainty (n_A) in one segment of the harvester.

Measurement HV@n = 30	* Type I	$n_{A,I}$	** Type II	$n_{A,II}$	*** Type III	$n_{A,III}$
U_0[V]@$Z_1 = \infty\ \Omega$	0.200	0.018	0.300	9.13×10^{-4}	0.800	6.39×10^{-4}
U_z[V]@$Z_{1,Re}$ = 150 Ω	0.0100	1.82×10^{-5}	0.0200	3.65×10^{-5}	0.500	0.0016
I_0[A]@$Z_1 = \infty\ \Omega$	0.00	0.00	0.00	0.00	0.00	0.00
I_z[A]@$Z_{1,Re}$ =150 Ω	6.66×10^{-5}	1.22×10^{-7}	1.33×10^{-4}	2.43×10^{-7}	0.500	1.06×10^{-5}
P_0[W]@$Z_1 = \infty\ \Omega$	0.00	0.00	0.00	0.00	0.00	0.00
P_z[W]@$Z_{1,Re}$ =150 Ω	6.66×10^{-7}	1.217×10^{-11}	2.66×10^{-6}	4.86×10^{-11}	0.00166	9.21×10^{-8}

* Type I according to Figure 1. ** Type II according to Figure 2. *** Type III according to Figure 3.

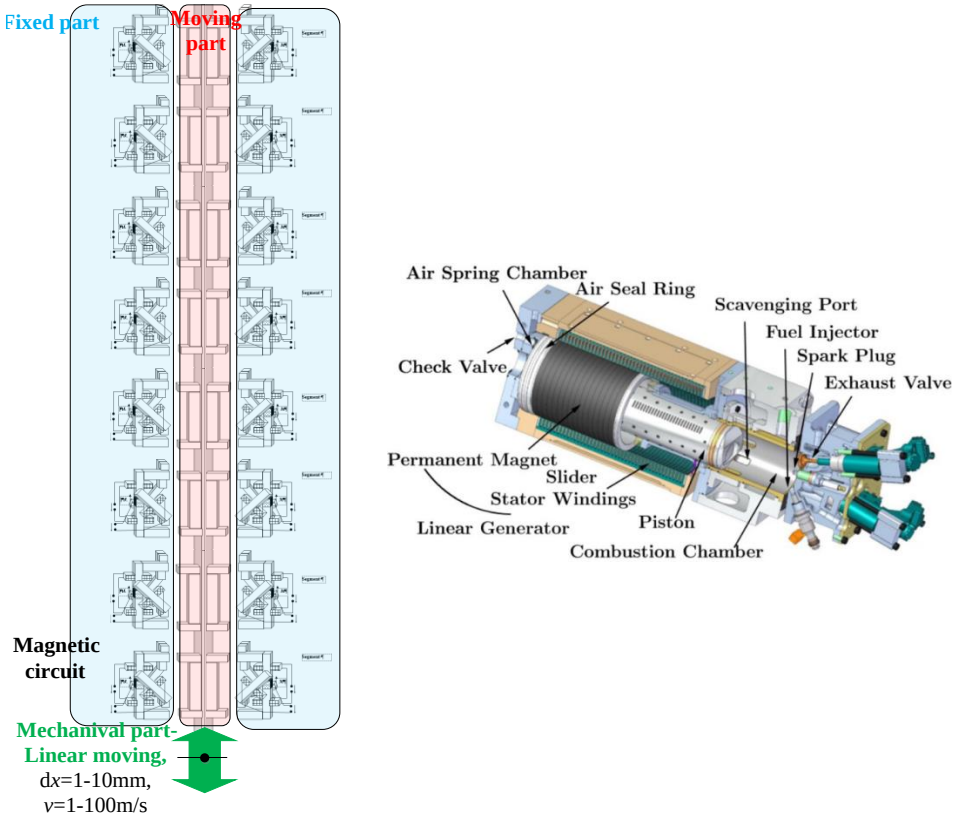

Figure 8. The concept of a periodically arranged harvester: (**a**) from segments with the required expected parameters, power in the band P = 10−10,000 W; (**b**) an example of the linear generator design [48].

5. Conclusions

Based on our experience with numerical models and related experiments with a microgenerator as a source of renewable energy, we have proposed the design of a powerful motion-excited linear generator to first approximate the expected results with a linear reciprocating engine driven by compressed gas. The design was modified to deliver high efficiency in converting kinetic energy into electricity, the performance having been expected based on previous experience [19,20].

Relevant experiments on a scale model demonstrated the feasibility of implementing such an energy conversion system as a harvester using a renewable form of energy. The numerical model and the analysis of the model parts significantly accelerated the geometrical design of the arrangement of the key parts of the electric generator. The selected variants of the magnetic circuit layout were experimentally verified, as was also an increase in the harvester yield through a double-acting arrangement of the magnetic circuit. After miniaturizing the cells and multiplying them, we evaluated the concept as a convenient alternative source of energy for both sensors in structures, including bridges, and motor vehicle systems. The experiments have proved that, in the harvester, the magnetic circuit configuration embodies the key factor for achieving the energy transformation yield; this fact has been largely neglected thus far. Further, changing the magnetic circuit, with a comparable electrical load, produces an up to 50-fold increase in the output voltage; at the given electrical load, this then indicates a 2500 times higher output power (Table 2, type I and type III @ $Z_{1,Re}$ = 150 Ω). Future research will focus on interfacing the harvester with sensor systems, completing the periodic arrangement of the segments, and measuring the overall efficiency of the generator.

The impact of the investigation and experimenting herein lies in characterizing an approach to arrange the magnetic circuit within the linear configuration of a generator in such a manner that a substantially higher volume of electricity is extracted under load and mechanical energy inputs that are equivalent to standard conditions (see Figure 3, type III). These relevant solutions, to the best of our knowledge, have not been fully considered or published to date.

Author Contributions: P.F. and J.Z. contributed to the theoretical part, numerical modeling, and design of the experiments, and they also co-wrote the paper; Z.S. and J.D. conceived and designed the experiments that allowed for the partial verification of the effects; and T.K. with R.K. modified the manuscript graphically and participated in evaluating the experiments. All authors have read and agreed to the published version of the manuscript.

Funding: The research was funded via the National Sustainability program, from grants BD 2023–2025, FEKT-S-23-8425. For the actual analyses and experiments, the infrastructure of the IET was utilized.

Data Availability Statement: Data are contained within the article.

Conflicts of Interest: The authors declare no conflicts of interest. The funding organizations had no role in the concept of the study; in the collection, analyses, or interpretation of the data; in the writing of the manuscript; or in the decision to publish the results.

References

1. Stratton, J.A. *Theory of Electromagnetic Field*; SNTL: Prague, Czech Republic, 1961.
2. Cawthorne, W.R. Optimization of a Brushless Permanent Magnet Linear Alternator for Use with a Linear Internal Combustion Engine. Ph.D. Thesis, Dissertations, and Problem Reports, 1999; p. 3160. Available online: https://researchrepository.wvu.edu/etd/3160 (accessed on 25 May 2022).
3. Jirků, T.; Fiala, P.; Kluge, M. Magnetic resonant harvesters and power management circuit for magnetic resonant harvesters. *Microsyst. Technol.* **2010**, *16*, 677–690. [CrossRef]
4. Cawthorne, W.R.; Famouri, P.; Chen, J.; Clark, N.N.; McDaniel, T.I.; Atkinson, R.J.; Nandkumar, S.; Atkinson, C.M.; Petreanu, S. Development of a linear alternator-engine for hybrid electric vehicle applications. *IEEE Trans. Veh. Technol.* **1999**, *48*, 1797–1802. [CrossRef]
5. Famouri, P.; Cawthorne, W.R.; Clark, N.; Nandkumar, S.; Atkinson, C.; Atkinson, R.; Petreanu, S. Design and testing of a novel linear alternator and engine system for remote electrical power generation. In Proceedings of the IEEE Engineering Society, Winter Meeting, New York, NY, USA, 31 January–4 February 1999; Volume 1, pp. 108–112.
6. Nor, K.M.; Arof, H.; Wijono. Design of a 5 kW tubular permanent magnet linear generator. In Proceedings of the 39th International Universities Power Engineering Conference, UPEC 2004, Bristol, UK, 6–8 September 2004; Volume 1, pp. 528–532.
7. Hernandez, I.; Segundo, J.; Gonzalez, X.; Luna, D.; Juarez, Z. Performance and power quality assessment of a linear electric generator focused on microgeneration applications. *Int. Trans. Electr. Energ. Syst.* **2017**, *27*, e2326. [CrossRef]
8. Fiala, P.; Szabo, Z.; Marcon, P.; Roubal, Z. Mini- and microgenerators applicable in the MEMS technology. In Proceedings of the SPIE—The International Society for Optical Engineering, San Diego, CA, USA, 6–10 August 2017; p. 10246. [CrossRef]
9. Atkinson, C.M.; Petreanu, S.; Clark, N.N.; Atkinson, R.J.; McDaniel, T.I.; Nandkumar, S.; Famouri, P. *Numerical Simulation of a Two-Stroke Linear Engine-Alternator Combination*; SAE Technical Papers; SAE International: Warrendale, PA, USA, 1999. [CrossRef]
10. Mikalsen, R.; Roskilly, A.P. Performance simulation of a spark ignited free-piston engine generator. *Appl. Therm. Eng.* **2008**, *28*, 1726–1733. [CrossRef]
11. Clark, N.N.; McDaniel, T.I.; Atkinson, R.J.; Nandkumar, S.; Atkinson, C.; Petreanu, S.; Famouri, P. Modeling and development of a linear engine. Paper No. 98-ICE-95. In Proceedings of the Spring Technical Conference, ASME, Fort Lauderdale, FL, USA, 26–29 April 1998.
12. Fredriksson, J.; Denbratt, I. *Simulation of a Two-Stroke Free Piston Engine. Paper No. 2004-01-187*; SAE International: Warrendale, PA, USA, 2004.
13. Van Blarigan, P.; Sandia National Laboratories. Advanced Internal Combustion Electrical Generator. In Proceedings of the 2001 DOE Hydrogen Program Review, NREL/CP-570-30535, Baltimore, MD, USA, 17–19 April 2001.
14. Pavelka, J. Analysis of combustion engine—Electric linear generator set operation. In Proceedings of the 13th International Power Electronics and Motion Control Conference (EPE/PEMC 2008), IEEE, Poznan, Poland, 1–3 September 2008; pp. 988–993. [CrossRef]
15. Mikalsen, R.; Roskilly, A.P. A review of free-piston engine history and applications. *Appl. Therm. Eng.* **2007**, *27*, 2339–2352. [CrossRef]
16. Virsik, R.; Heron, A. Free piston linear generator in comparison to other range-extender technologies. *World Electr. Veh. J.* **2013**, *6*, 426–435. [CrossRef]

17. Lim, O.; Hung, N.B.; Iida, N. A power generation study of a power pack based on operating parameters of the linear engine fuelled with propane. *Energy Procedia* **2014**, *61*, 1581–1584. [CrossRef]
18. Szabo, Z.; Fiala, P.; Dohnal, P. Magnetic circuit modifications in resonant vibration harvesters. *Mech. Syst. Signal Process.* **2018**, *99*, 832–845. [CrossRef]
19. Zukal, J.; Fiala, P.; Szabó, Z.; Dedková, J.; Pernica, R. Coupled numerical model of vibration-based harvester. *Appl. Sci.* **2020**, *10*, 2725. [CrossRef]
20. Szabó, Z.; Fiala, P.; Zukal, J.; Dědková, J.; Dohnal, P. Optimal structural design of a magnetic circuit for vibration harvesters applicable in MEMS. *Symmetry* **2020**, *12*, 110. [CrossRef]
21. Zukal, J.; Szabo, Z.; Pernica, R.; Kadlec, R.; Dedkova, J.; Klima, M.; Fiala, P. Designing a Robust Model of a Linear Motion-driven Harvester. In Proceedings of the Photonics & Electromagnetics Research Symposium (PIERS), Prague, Czech Republic, 3–6 July 2023; pp. 732–738. [CrossRef]
22. Schillingmann, H.; Maurus, Q.; Henke, M. Linear generator design for a free-piston engine with high force density. In Proceedings of the 12th International Symposium on Linear Drives for Industry Applications, LDIA, Neuchatel, Switzerland, 1–3 July 2019. [CrossRef]
23. Baker, N.J.; Sa Jalal, A.; Wang, J.; Korbekandi, R.M. Experimental comparison of two linear machines developed for the free piston engine. *J. Eng.* **2019**, 4406–4410. [CrossRef]
24. Baker, N.J.; Korbekandi, R.M.; Wu, D.; Jalal, A.S. An investigation of short translator linear machines for use in a free piston engine. In Proceedings of the IEEE International Electric Machines and Drives Conference, IEMDC, San Diego, CA, USA, 12–15 May 2019; pp. 68–73. [CrossRef]
25. Subramanian, J.; Heiskell, G.; Mahmudzadeh, F.; Famouri, P. Study of radial and axial magnets for linear alternator—Free piston engine system. In Proceedings of the 2017 North American Power Symposium, NAPS 2017, Morgantown, WV, USA, 17–19 September 2017. [CrossRef]
26. Hansson, J. Analysis and Control of a Hybrid Vehicle Powered by a Free-Piston Energy Converter, Electrical Machines and Power Electronics. Licentiate Thesis, School of Electrical Engineering, Royal Institute of Technology (KTH), Stockholm, Sweden, 2006.
27. Kulkarni, S.; Koukharenko, E.; Torah, R.; Tudor, M.J.; Beeby, S.; O'Donnell, T. Design, fabrication and test of integrated micro-scale vibration-based electromagnetic generator. *Sens. Actuators A Phys.* **2008**, *145–146*, 336–342. [CrossRef]
28. Beeby, S.P.; Torah, R.N.; Torah, M.J.; O' Donnell, T.; Saha, C.R.; Roy, S. A microelectromagnetic generator for vibration energy harvesting. *J. Micromech. Microeng.* **2007**, *17*, 1257–1265. [CrossRef]
29. Zhu, D.; Roberts, S.; Tudor, M.J.; Beeby, S.P. Design and experimental characterization of a tunable vibration-based electromagnetic microgenerator. *Sens. Actuators A Phys.* **2010**, *158*, 284–293. [CrossRef]
30. Elvin, N.G.; Elvin, A.A. An experimentally validated electromagnetic energy harvester. *J. Sound. Vib.* **2011**, *330*, 2314–2324. [CrossRef]
31. Wang, P.H.; Dai, X.H.; Fang, D.M.; Zhao, X.L. Design, fabrication and performance of a new vibration-based electromagnetic micro power generator. *Microelectron. J.* **2007**, *38*, 1175–1180. [CrossRef]
32. Yang, J.; Yu, Q.; Zhao, J.; Zhao, N.; Wen, Y.; Li, P.; Qiu, J. Design and optimization of a biaxial vibration-driven electromagnetic generator. *J. Appl. Phys.* **2014**, *116*, 114506. [CrossRef]
33. Lee, B.C.; Rahman, M.A.; Hyun, S.; Chung, S.G. Low frequency driven electromagnetic energy harvester for self-powered system. *Smart Mater. Struct.* **2012**, *21*, 125024. [CrossRef]
34. Quinn, J.B.; Waldmann, T.; Richter, K.; Kasper, M.; Wohlfahrt-Mehrens, M. Energy Density of Cylindrical Li-Ion Cells: A Comparison of Commercial 18650 to the 21700 Cells. *J. Electrochem. Soc.* **2018**, *165*, A3284–A3291. [CrossRef]
35. Liu, C.; Yu, Z.; Liu, C.; Yu, Z.; Neff, D.; Zhamu, A.; Jang, B.Z. Graphene-Based Supercapacitor with an Ultrahigh Energy Density. *Nano Lett.* **2010**, *10*, 4863–4868. [CrossRef]
36. Yamanaka, Y.; Nirei, M.; Sato, M.; Murata, H.; Yinggang, B.; Mizuno, T. Design of linear synchronous generator suitable for free-piston engine linear generator system. In Proceedings of the 11th International Symposium on Linear Drives for Industry Applications (LDIA), IEEE, Osaka, Japan, 6–8 February 2017; pp. 1–4. [CrossRef]
37. Subramanian, J.; Mahmudzadeh, F.; Bade, M.; Famouri, P. Simulation and Experimental Validation of Equivalent Circuit Parameters and Core Loss in a Tubular Permanent Magnet Linear Generator for Free Piston Engine Applications. In Proceedings of the IEEE International Electric Machines & Drives Conference (IEMDC), IEEE, San Diego, CA, USA, 12–15 May 2019; pp. 57–62. [CrossRef]
38. Zhang, X.; Cooke, K.B.; Kos, J. Modeling and simulation of a hybrid-engine. In Proceedings of the IEEE WESCANEX 97 Communications, Power and Computing. Conference Proceedings, Winnipeg, MB, Canada, 22–23 May 1997; pp. 286–291. [CrossRef]
39. Fazal, I.; Karsiti, M.N.; Zulkifli, S.A.; Ibrahim, T.; Rao, K.S.R. Modeling and simulation of a moving-coil linear generator. In Proceedings of the Advanced Systems (ICIAS 2010), IEEE, Kuala Lumpur, Malaysia, 15–17 June 2010; pp. 1–5. [CrossRef]
40. Graef, M.; Treffinger, P.; Pohl, S.-E.; Rinderknecht, F. Investigation of a high efficient Free Piston Linear Generator with variable Stroke and variable Compression Ratio A new Approach for Free Piston Engines. *World Electr. Veh. J.* **2007**, *1*, 116–120. [CrossRef]
41. Tikkanen, R.S.; Vilenius, M. Hydraulic free piston engine—Challenge for control. In Proceedings of the 1999 European Control Conference (ECC), IEEE, Karlsruhe, Germany, 31 August–3 September 1999; pp. 2943–2948. [CrossRef]

42. Zou, H.; Wang, M.; Tang, M.; Li, C.; Tian, C. Experimental investigation and performance analysis of a direct-driven linear generator. *Energy Procedia* **2017**, *142*, 284–290. [CrossRef]
43. Seo, U.-J.; Riemer, B.; Appunn, R.; Hameyer, K. Design considerations of a linear generator for a range extender application. *Arch. Electr. Eng.* **2015**, *64*, 581–592. [CrossRef]
44. Takahara, K.; Ohsaki, S.; Itoh, Y.; Ohyama, K.; Kawaguchi, H. Characteristic analysis and trial manufacture of permanent-magnetic type linear generator. *Electr. Eng. Jpn.* **2008**, *166*, 94–100. [CrossRef]
45. Nguyen, V.T.; Ta, Q.T.H.; Nguyen, P.K.T. Artificial intelligence-based modeling and optimization of microbial electrolysis cell-assisted anaerobic digestion fed with alkaline-pretreated waste-activated sludge. *Biochem. Eng. J.* **2022**, *187*. [CrossRef]
46. Talib, N.H.H.A.; Salleh, H.; Youn, B.D.; Resali, M.S.M. Comprehensive Review on Effective Strategies and Key Factors for High Performance Piezoelectric Energy Harvester at Low Frequency. *Int. J. Automot. Mech. Eng.* **2019**, *16*, 7181–7210. [CrossRef]
47. ANSYS. 1990–2023, USA. Available online: www.ansys.com (accessed on 12 November 2023).
48. Available online: https://www.greencarcongress.com/2016/05/20160506-toyotafpeg.html (accessed on 8 January 2024).